# Water Is The Enemy: Developing Hydrothermally Stable Ti-PMO Catalysts for Sustainable Aviation Fuel Synthesis

**Abstract**

Sustainable aviation fuels (SAFs) can be made from biomass-derived molecules, but the chemical step that builds the fuel precursor needs a catalyst that can survive the reaction conditions and maintain the same or improved level of catalytic activity [17, 18]. The current standard catalyst, titanium grafted onto a silica support called SBA-15, works well but produces water as a by-product of the reaction it catalyzes, and that water slowly breaks the catalyst down over time [1, 5]. This research tests whether a different kind of support, called a periodic mesoporous organosilica (PMO), can fix that problem while still retaining a comparable or improved level of catalytic activity [2, 3, 4]. We built a new catalyst, titanium-grafted PMO (Ti-PMO), and confirmed its structure using several techniques. We then tested how well it survives simulated hydrothermal (hot and wet) ageing conditions compared to titanium-grafted SBA-15 [10, 13], and tested its photocatalytic activity using a dye-degradation reaction as a stand-in test [14, 16, 20]. The PMO support kept its ordered internal structure after 24 hours of hydrothermal treatment, while the SBA-15 support did not. The Ti-PMO catalyst also degraded 1.78 times more dye per mole of titanium than Ti-SBA15, despite containing 2.5 times less titanium overall, meaning each titanium site in the PMO catalyst is roughly 2.4 times more active. These results suggest that pairing titanium active sites with a PMO support could produce catalysts that last longer under real operating conditions, which matters directly for the cost and practicality of producing SAF at scale [5].

## 1. Introduction

### 1.1 Why do we need to create sustainable aviation fuels?

Aviation is hard to decarbonize because planes cannot run on batteries. Batteries don't have the required energy density and are too bulky to carry on long-haul flights [17, 18, 19]. Sustainable aviation fuel (SAF) is fuel made from renewable feedstocks (like plant-derived molecules) instead of crude oil, designed to be a drop-in replacement for conventional jet fuel [17]. Making SAF at the scale aviation needs requires chemical reactions that build small biomass molecules into larger, fuel-like molecules, and those reactions need catalysts to happen efficiently and cheaply [18, 19].

One important reaction in this process is called an **aldol condensation**. In simple terms, this is a reaction where two molecules are stitched together, with a water molecule released as a by-product [8, 9]. In our system, two biomass-derived molecules, cyclopentanone (CPO) and

furfural (FAL), are joined together using this reaction [6]. The first stitching step produces an intermediate called FCp-OH, which then loses a water molecule to form FCp. FCp can react with a second furfural molecule in the same way to form F2Cp, a larger molecule that's a better precursor for jet fuel [6, 7]. This is called a **cross-condensation** because it links two different starting molecules rather than two copies of the same one.

### 1.2 The current catalyst and its problem

The catalyst typically used for this reaction is **titanium grafted onto SBA-15** [1]. SBA-15 is a type of silica that's manufactured with a highly ordered network of tiny, uniform pores running through it. This structure gives it a huge internal surface area, which is valuable because it means you can pack a lot of catalytic activity into a small amount of material. "Grafting" titanium onto it means chemically attaching titanium atoms to the silica's surface, where they act as **Lewis acid sites** [1]. A Lewis acid is a chemical species that can accept a pair of electrons from another molecule, which is the specific chemical trick needed to catalyze the aldol condensation described above.

This catalyst is also **photocatalytically enhanced**, meaning its activity is boosted by exposure to light, which points to the titanium sites being both Lewis acid catalysts and light-activated catalysts [1, 20].

The problem is that the aldol condensation reaction itself produces water as a by-product, and that water accelerates the catalyst's own degradation over time through hydrolysis of the Ti-O-Si framework bonds, forming Ti-OH2 or Ti(OH)2, which pulls titanium out of its catalytically active sites and causes it to aggregate into inactive extra-framework species, while also collapsing the mesoporous silica structure that supports it. So, this means the catalyst needs to be replaced or regenerated more often, which raises the cost of producing fuel at scale.

### 1.3 The proposed fix: graft titania onto periodic mesoporous organosilicas (PMOs)

A **periodic mesoporous organosilica**, or PMO, is a material similar to SBA-15 in that it also has an ordered network of nanoscale pores, but with a key difference: instead of being built entirely from silicon-oxygen bonds, part of its structural framework is made from organic molecular "bridges", in our case, a benzene group woven directly into the pore walls [4, 12, 21]. This has two useful consequences:

1. **Increased hydrophobicity.** "Hydrophobic" means water-repelling. Because part of the PMO's structure is organic rather than purely silica, it repels water more than SBA-15 does [11, 13]. Since water is the very thing degrading the current catalyst, a more water-repelling support could directly address the stability problem [2, 3].
2. **Potential for improved charge separation.** The aromatic (ring-shaped) organic framework may help electrons behave differently near the titanium sites when light hits the catalyst, which could make the photocatalytic activity more efficient [14, 15]. However, further research is needed to confirm the extent to which this ligand-to-metal

charge transfer, rather than other factors, drives the observed improvement in catalytic activity.

The core idea of this work, then, is: **can we combine the water-repelling, hydrothermally stable framework of a PMO with the catalytically active titanium sites currently used on SBA-15, to get a catalyst that lasts longer under real reaction conditions?**

### 1.4 Objectives

This paper addresses two specific questions:

- Objective 1: Does a PMO actually survive hydrothermal ageing better than SBA-15, the current industry-standard support?
- Objective 2: Can titanium be successfully grafted onto a PMO to make a new catalyst (Ti-PMO), and if so, how does its catalytic activity compare to the current Ti-SBA15 catalyst?

## 2. Materials and Methods

### 2.1 Making the supports

Both SBA-15 (a purely silica mesoporous support) and the phenylene-bridged PMO were synthesized using a templating method, adapted from a published protocol by Sánchez-Vázquez et al [2]. Templating involves a surfactant (a soap-like molecule) being dissolved in water, where it self-assembles into a scaffold of tiny rod-like structures. A silica-forming precursor is then added around this scaffold. As it solidifies, it forms a solid material with the surfactant rods embedded inside it like the pattern in a mold, and once the surfactant is later removed (see below), what's left behind is a solid riddled with the nanoscale channels, which are the pores that give these materials their large internal surface area.

**Step-by-step procedure:**

1. **Dissolving the template:** 3.217 g P-123 (the template) was dissolved in a mixture of 103.0 mL H2O and 1.07 mL of 37% HCl
2. **Adding the silica-forming precursor:**
    a. For the 100% BTSB PMO (referred to as ‘PMO’), 6.700 g of BTSB (1,4-bis(triethoxysilyl)benzene — a molecule where a benzene ring, a hexagonal carbon ring structure, sits between two silicon-containing groups) was added to the P123 solution [12]. Because BTSB contributes both the silicon and the organic phenylene bridge in a single molecule, using 100% BTSB (with no separate silica precursor) produces a framework where the phenylene groups are built directly into the pore walls throughout the whole material [4].

    b. For SBA-15, 3.46 g of TEOS (tetraethyl orthosilicate, which is a conventional, purely silicon-based precursor with no organic component) was used instead. This produces an equivalent pore structure but is made entirely of silica, with no organic bridges
    c. Both mixtures were left to stir overnight after the precursor was added, allowing the silica (or silica-organic) network to form around the P123 scaffold.
3. **Aging:** The mixtures were heated to 130 °C for 24 hours in a sealed vessel. This aging step allows the forming solid to fully condense and rigidify around the surfactant template, locking in the pore structure.
4. **Isolating the solid:** The resulting solid product was collected by vacuum filtration and washed three times with deionized water to remove unreacted chemicals.
5. **Removing the template:** At this stage, the P123 surfactant scaffold is still physically trapped inside the pores. So, it needs to be removed to leave the pores empty and usable
    a. For the 100% BTSB PMO, this was done by refluxing the solid twice, for 24 hours each time, in a 1:1 mixture of ethanol and 1 M HCl. The acidic ethanol dissolves the surfactant out of the pores without damaging the silica or PMO framework itself.
    b. For SBA-15, the template was extracted by calcining the material for 24 hours at 550 C, since the vaporizing point of organic-containing P-123 is much lower than the vaporizing point of the purely silica support

**2.2 Grafting titanium**

Titanium was introduced onto both the PMO and the SBA-15 using a post-synthesis grafting method, meaning the titanium is added after the support material already exists [1, 16]. The titanium precursor (titanium butoxide) was reacted directly with the silanol (Si-OH) groups naturally present on the pore surfaces.

**Step-by-step procedure:**

1. 0.2 g of the 100% BTSB PMO support was dissolved/suspended in 30 mL of anhydrous (water-free) toluene, under an argon (Ar) atmosphere. Both conditions are necessary because the titanium precursor used in the next step reacts readily with water. So, an anhydrous solvent and an inert argon atmosphere (which excludes moisture and oxygen from the air) prevent the titanium from reacting prematurely with ambient water instead of with the support's surface.
2. 0.022 mL of triethylamine (TEA) was added and stirred in. TEA acts as a base here, helping to activate the surface silanol groups and neutralize the by-product acid generated during the grafting reaction, which helps the titanium attach efficiently.
3. 0.19 mL of titanium(IV) butoxide was added, and the mixture was refluxed (heated at boiling point under a condenser) overnight at 85 °C. During this step, the titanium butoxide reacts with the surface Si–OH groups, releasing butanol as a by-product and leaving titanium atoms covalently anchored to the support's surface. This is what

produces the isolated, surface-grafted Ti(IV) sites confirmed later by XPS (Section 3.1) [16].

The same procedure was used to graft titanium onto SBA-15, producing Ti-SBA-15 for comparison.

### 2.3 Hydrothermal ageing protocol (autoclave experiment)

To directly test how each support responds to hydrothermal stress, SBA-15 and the 100% BTSB PMO were each subjected to a controlled ageing experiment using an autoclave (a sealed vessel that can hold water under both elevated temperature and the resulting elevated pressure, since sealed water heated above 100 °C generates pressure as it tries to turn to steam) [10, 11, 13].

**Step-by-step procedure:**

1. 0.20 g of catalyst was weighed into the PTFE (a chemically inert plastic, often known by the brand name Teflon) liner of a 50 mL autoclave. The PTFE liner protects the metal autoclave body from corrosion and prevents the catalyst from picking up any contamination from the vessel itself.
2. 20 mL of deionized water was added to the same liner, fully immersing the catalyst.
3. The sealed autoclave was placed in a furnace and heated to 150 °C. Separate samples were treated for **1 hour, 6 hours, and 24 hours**, allowing degradation to be tracked across a time series rather than only comparing a single "before" and "after" point.

At each time point, the solid catalyst was recovered by vacuum filtration and analyzed by XRD to track any structural changes as a function of ageing time. This time-resolved approach (1 h, 6 h, 24 h) is what allows the ex-situ XRD comparisons in Section 3.2 to show not just whether degradation happens, but roughly how quickly it develops.

### 2.4 Characterization Techniques

We used several complementary techniques to confirm what the catalyst actually is and how it changes under ageing. Each is explained here in plain terms so the results in Section 3 make sense without technical background:

- **X-ray diffraction (XRD)**: shines X-rays at a sample and measures how they scatter off its internal structure. Regularly repeating (ordered) structures produce sharp peaks at specific angles; disordered structures produce broad, featureless humps. This is how we tell whether the material's pore structure survived ageing.
- **X-ray photoelectron spectroscopy (XPS)**: measures the elements present at a material's surface and, crucially, the chemical environment those elements are in (for example, whether titanium is bonded mainly to silicon-oxygen groups versus existing as bulk titanium dioxide) [1, 16].

- **Fourier-transform infrared spectroscopy (FTIR)**: identifies which chemical bonds are present in a material by measuring which wavelengths of infrared light it absorbs. Different bond types (like the aromatic C–H bonds in the phenylene bridge) absorb at characteristic wavelengths, so this confirms which chemical groups survived processing.
- **Reflection electron energy loss spectroscopy (REELS)**: a surface-sensitive technique that reveals information about a material's electronic structure. We used it to check whether grafting titanium onto the PMO, or ageing the PMO, changed its underlying electronic character.
- **Scanning electron microscopy (SEM)**: takes a highly magnified image of the material's surface using a focused beam of electrons, letting us directly see particle morphology.
- **Energy-dispersive X-ray spectroscopy (EDX)**: measures the elemental composition of a sample, giving us the percentage of titanium present, among other elements.
- **Thermogravimetric Analysis (TGA)**: measures weight loss as a sample is heated, useful for confirming organic content and thermal stability

**2.5 Photocatalytic Activity Testing (Rhodamine B assay)**

Photocatalytic activity was tested using the degradation of Rhodamine B (RhB), an organic dye, as a probe reaction [14, 15, 20]. This is a standard, well-established test used across catalysis research: RhB has a strong, easily measured color, so tracking how much of it breaks down over time under light exposure gives a simple, reproducible way to compare the light-driven activity of different catalysts, without needing to run the (much more complex) actual SAF-forming reaction for every screening test. RhB degradation is not the target reaction for SAF production, it is only a diagnostic tool for characterizing how active the titanium sites are.

**Step-by-step procedure:**

1. 0.2 g of catalyst (anatase, rutile, P25, Ti-SBA-15, or Ti-PMO) was added to 20 mL of an 8 mg/L RhB solution.
2. The mixture was placed in a sealed, dark box for 30 minutes under magnetic stirring. This dark, stirred period is a standard step in photocatalysis testing: it allows the system to reach adsorption-desorption equilibrium, meaning the point where dye molecules are sticking to and detaching from the catalyst's surface at an equal, steady rate. This matters because if testing began immediately under light, some of the apparent "degradation" measured early on would actually just be dye physically adsorbing onto the catalyst surface rather than being chemically broken down. The dark equilibration step separates out that adsorption effect so the light-driven reaction can be measured on its own.
3. A solar simulator (a lamp designed to mimic the spectrum of natural sunlight, used so that photocatalytic results are relevant to real-world, light-driven conditions) was positioned 8.45 cm from the solution and operated at a current of 7.45 A. The sample was then irradiated continuously.
4. Small aliquots of the irradiated solution were taken at 0, 2, 5, 10, 15, 30, 60, and 90 minutes.

5. The RhB concentration remaining in each aliquot was measured at 554 nm using UV-Vis spectrophotometry, a technique that measures how much light of specific wavelengths a solution absorbs. Since RhB has a strong, characteristic absorbance, the drop in absorbance over time directly tracks how much dye has been degraded.

This time-resolved sampling (eight points across 90 minutes, rather than a single before/after measurement) is what allows both the initial rate and the overall turnover frequency (TOF) values reported in Section 3.3 to be calculated, since both require tracking how conversion changes over time rather than a single endpoint.

## 3. Results and Discussion

### 3.1 Objective 1: Is the PMO support more hydrothermally stable than SBA-15?

Yes!

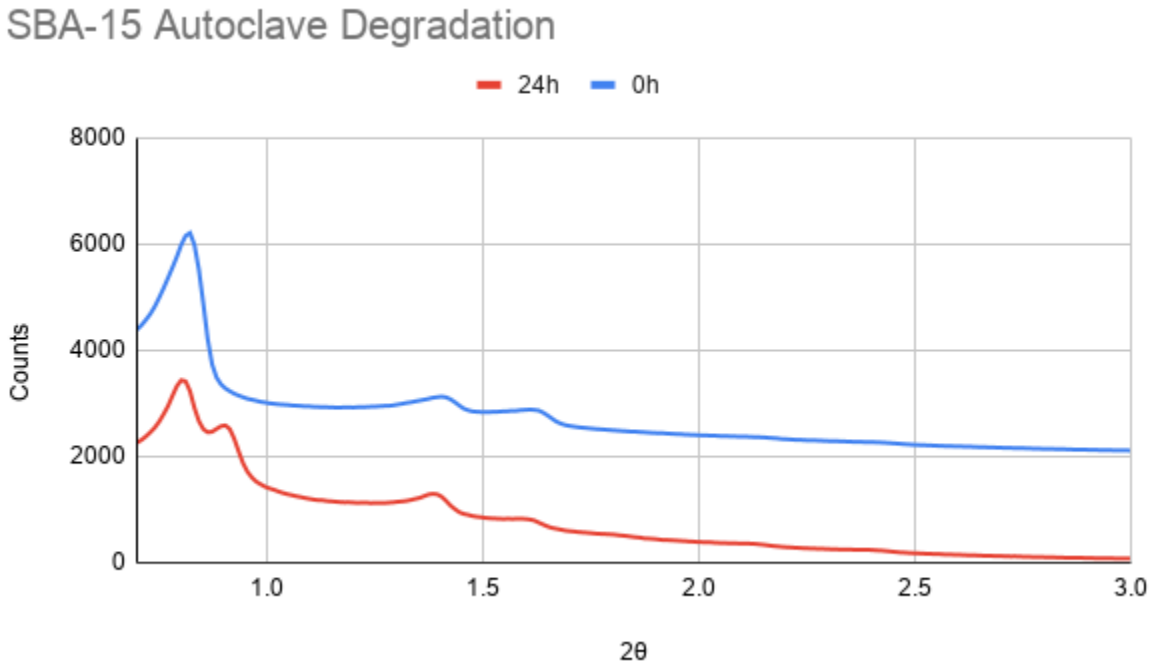


**Figure 1.** Low-angle XRD patterns of SBA-15 before (0h) and after (24h) hydrothermal treatment in an autoclave.

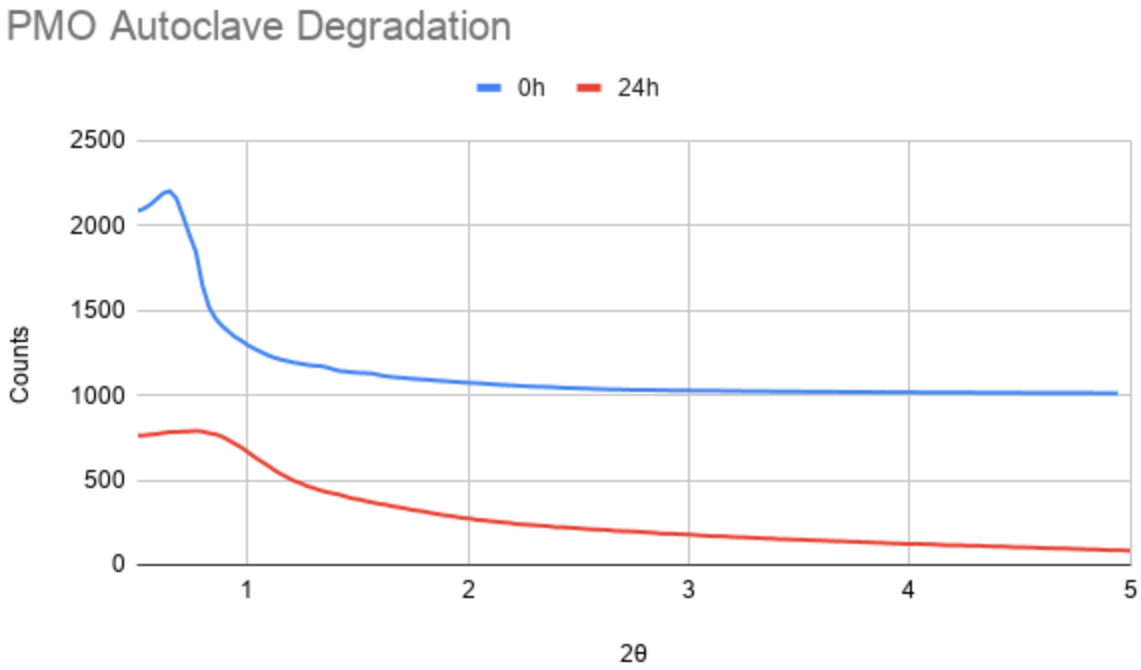


**Figure 2.** Low-angle XRD patterns of periodic mesoporous organosilica (PMO) before (0h) and after (24h) hydrothermal treatment in an autoclave.

Comparing XRD patterns of SBA-15 before (0h) and after (24h) hydrothermal treatment showed that SBA-15 loses its higher-order diffraction peaks (specifically ones called the (110) and (200) peaks) after ageing [10, 13]. These particular peaks can only appear if the material's pores are arranged with long-range hexagonal periodicity, meaning the pores are arranged in a large-scale repeating honeycomb pattern across the whole material. The disappearance of these peaks after 24 hours tells us that hydrothermal treatment destroys this large-scale order in SBA-15, even though a related peak (the (100) peak, which splits into two components) survives, showing that some smaller-scale, short-range order remains even as the big-picture structure collapses.

By contrast, the 100% BTSB PMO retained its periodic order after the same 24-hour treatment. We attribute this directly to the organic phenylene bridge: because part of the framework is hydrophobic organic material rather than purely silica, the PMO resists the structural breakdown that water causes in pure-silica SBA-15 [11, 13].

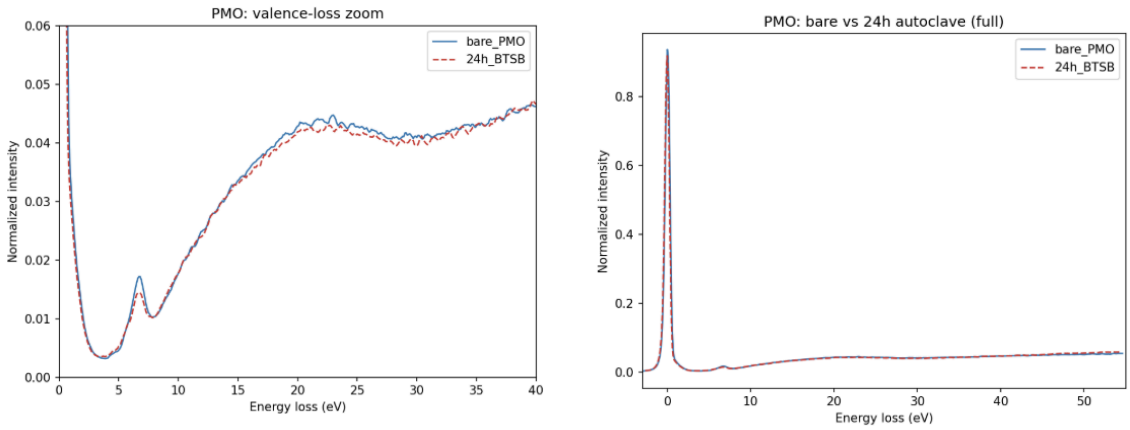


**Figure 3.** REELS spectra of bare PMO and 24h-autoclaved PMO (BTSB), showing (left) the valence-loss region and (right) the full survey-loss spectrum.

The near-identical peak positions and shapes of the REELS measurements after 24h on the PMO before and after hydrothermal treatment showed no shift in electronic structure, reinforcing that the material's surface chemistry remains intact through ageing.

### 3.2 Objective 2: Was the Ti-PMO successfully synthesized?

Yes!

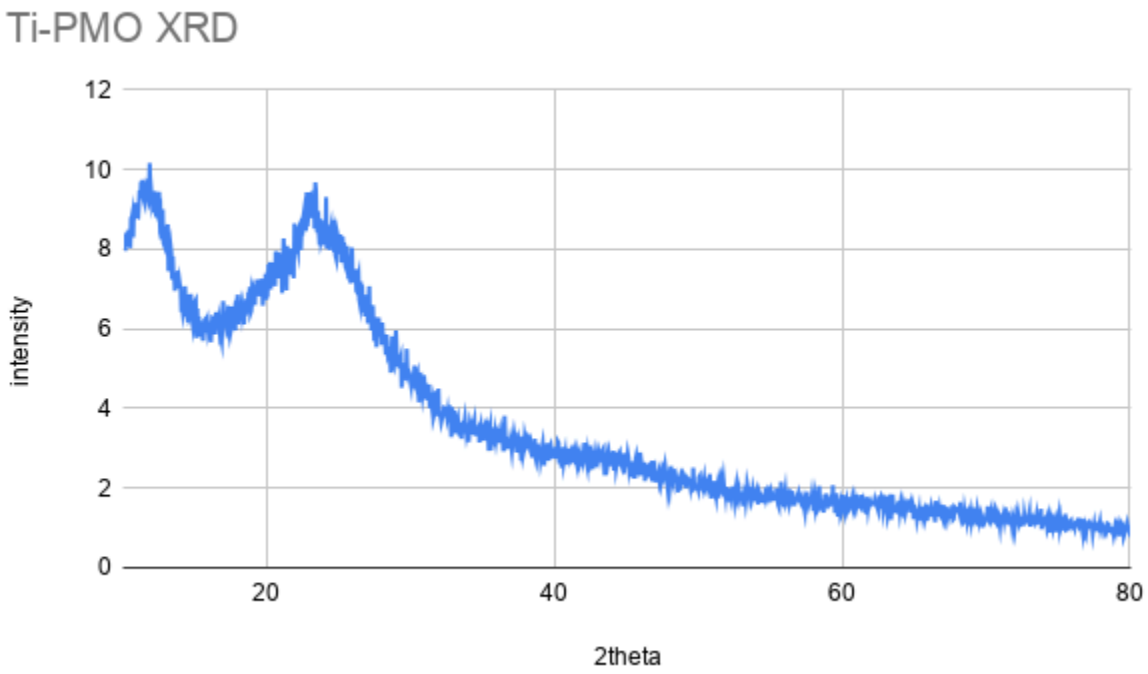


**Figure 4.** Wide-angle XRD pattern of Ti-PMO. Note that there is an absence of sharp Bragg reflections and the presence of only broad diffuse humps (~10-25° 2θ).

**XRD** showed a broad peak between 8–12° 2θ, which is the signature of an ordered mesopore structure. This confirms the material retains the repeating pore arrangement rather than being an amorphous mix. A second broad feature around 23° 2θ reflects the short-range order of the amorphous silica itself. Critically, there were no sharp peaks anywhere between 25° and 80° 2θ, which is where crystalline titanium dioxide (in either its anatase or rutile crystal forms) would show up. Their absence tells us the titanium was successfully grafted as isolated, molecularly dispersed sites rather than clumping together into separate TiO2 particles [16, 20].

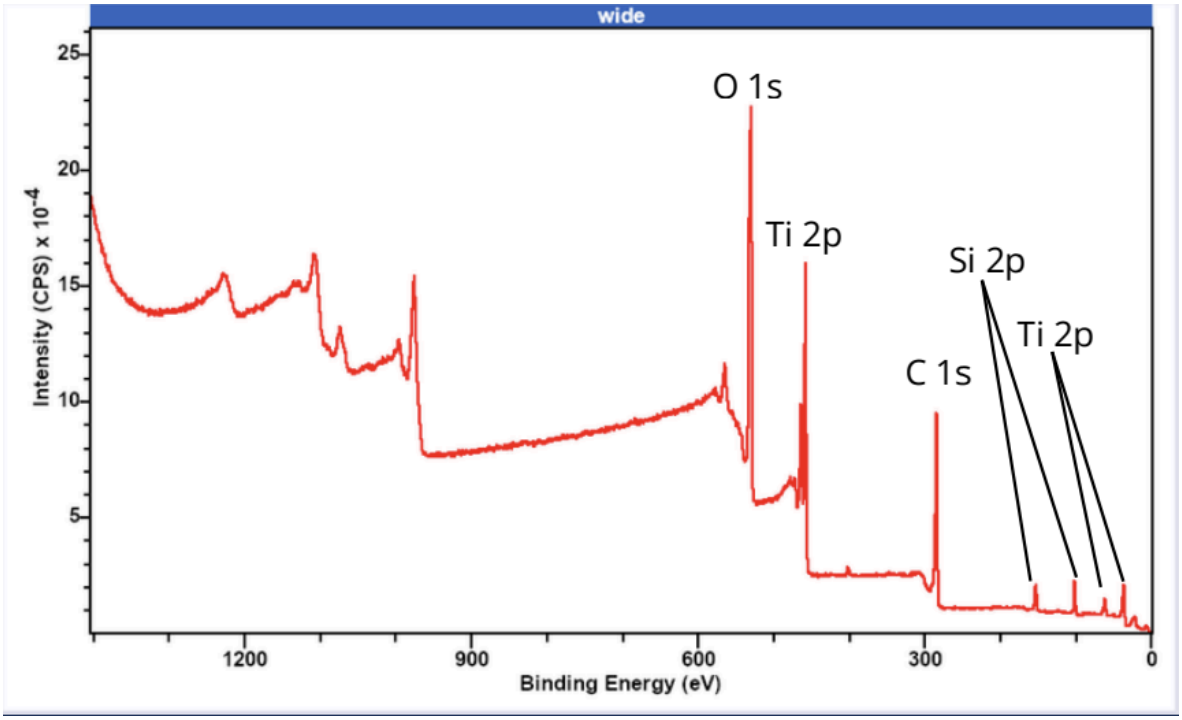


**Figure 5.** XPS survey spectrum of Ti-PMO with O 1s, Ti 2p, C 1s, and Si 2p core-level peaks identified.

**XPS** confirmed the presence of titanium, oxygen, silicon, and carbon at the surface, as expected. The titanium 2p3/2 signal (a specific electron energy peak used to identify titanium's chemical environment) appeared at a slightly higher binding energy than is typical for pure TiO2, in the range of 459-459.5 eV. This shift indicates the titanium is sitting in a Si-O-Ti environment (bonded to the silica framework) rather than existing as bulk titanium oxide, since that environment is more electron-withdrawing than the Ti-O-Ti bonding found in pure TiO2 [1, 16].

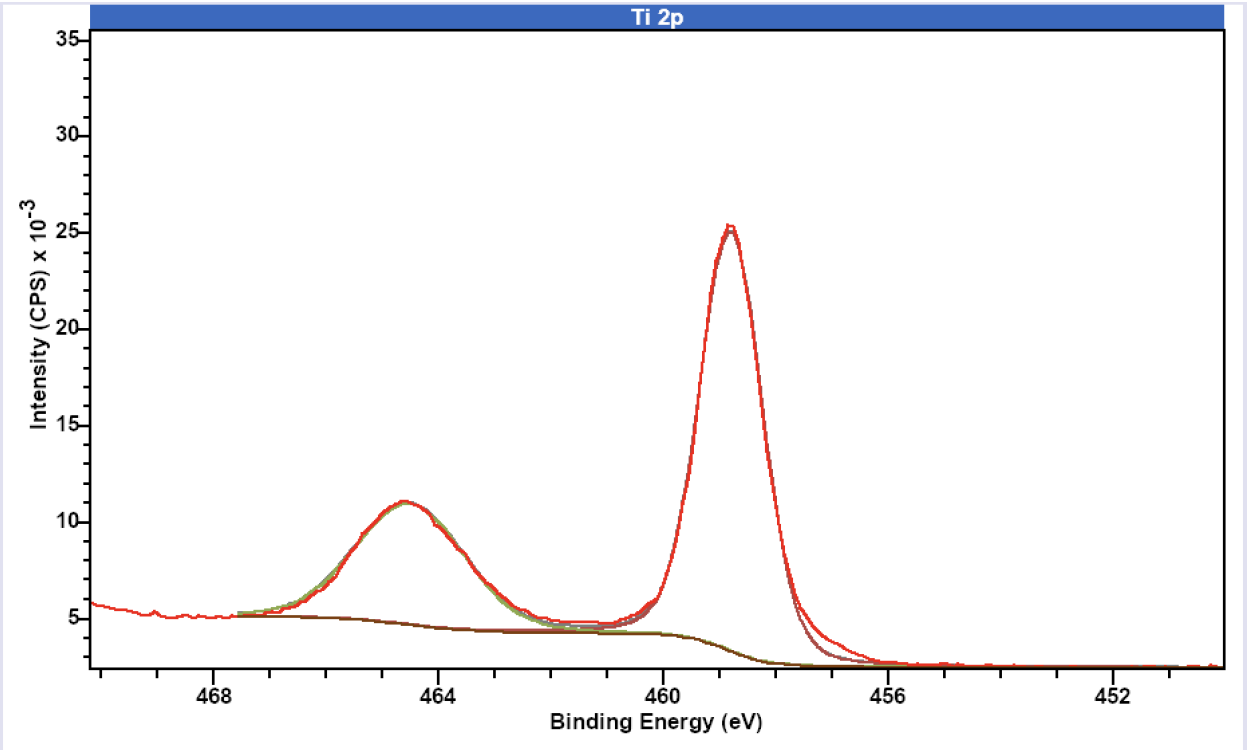


**Figure 6.** High-resolution XPS spectrum of the Ti 2p region, fitted with a spin-orbit doublet at binding energies consistent with Ti(IV) (Ti 2p3/2 and Ti 2p1/2)

The spacing between the Ti 2p3/2 and Ti 2p1/2 peaks (about 5.7 eV, with the second peak at half the intensity of the first) and the absence of a lower-energy "shoulder" that would indicate Ti(III) confirms the titanium is fully in its Ti(IV) oxidation state.

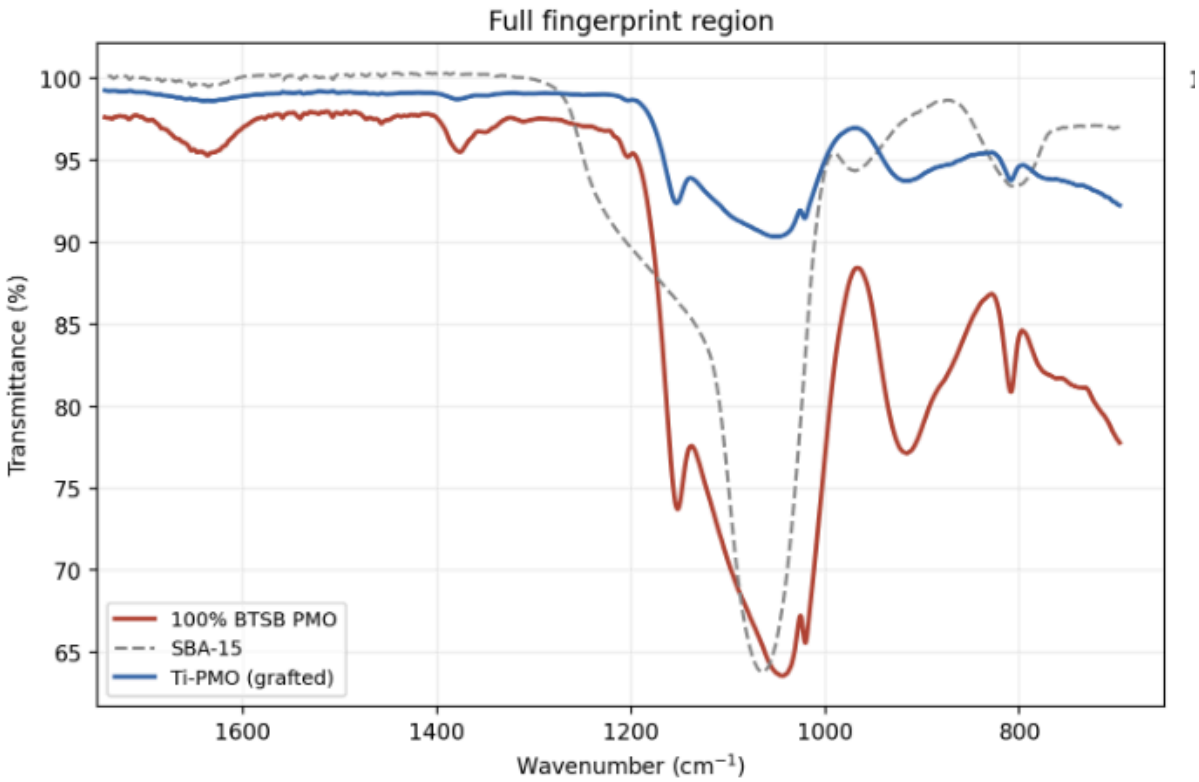


**Figure 7.** FTIR spectra in the fingerprint region comparing 100% BTSB PMO, unfunctionalized SBA-15, and Ti-grafted PMO.

**FTIR** showed aromatic C-H bending bands around 1080 $cm^{-1}$ (a signature vibration of the benzene ring structure) present in both the bare BTSB-PMO and the Ti-grafted PMO, but absent in SBA-15 [4, 12]. This confirms that the organic phenylene bridge survives the titanium grafting process intact.

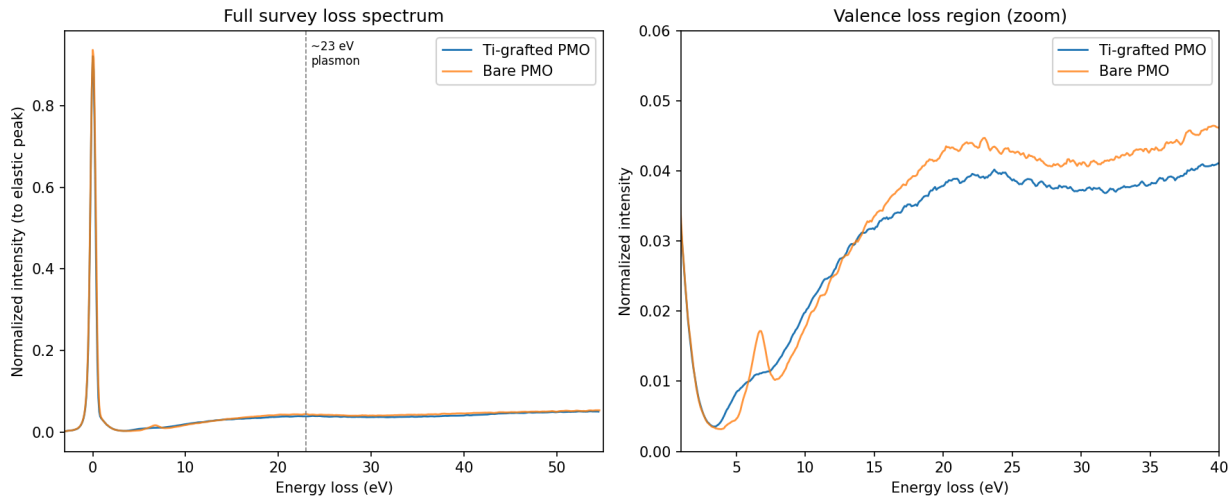


**Figure 8.** REELS spectra comparing Ti-grafted and bare PMO: (left) full survey-loss spectrum with the ~23 eV silica plasmon marked, and (right) zoomed valence-loss region.

**REELS** showed no shift in the surface electronic structure between the bare PMO and the Ti-grafted PMO, indicating that grafting titanium onto the surface doesn't disrupt the underlying electronic character of the support itself. Both samples show an elastic peak at 1004.5–1004.6 eV kinetic energy and a dominant valence-loss feature at ~23 eV.

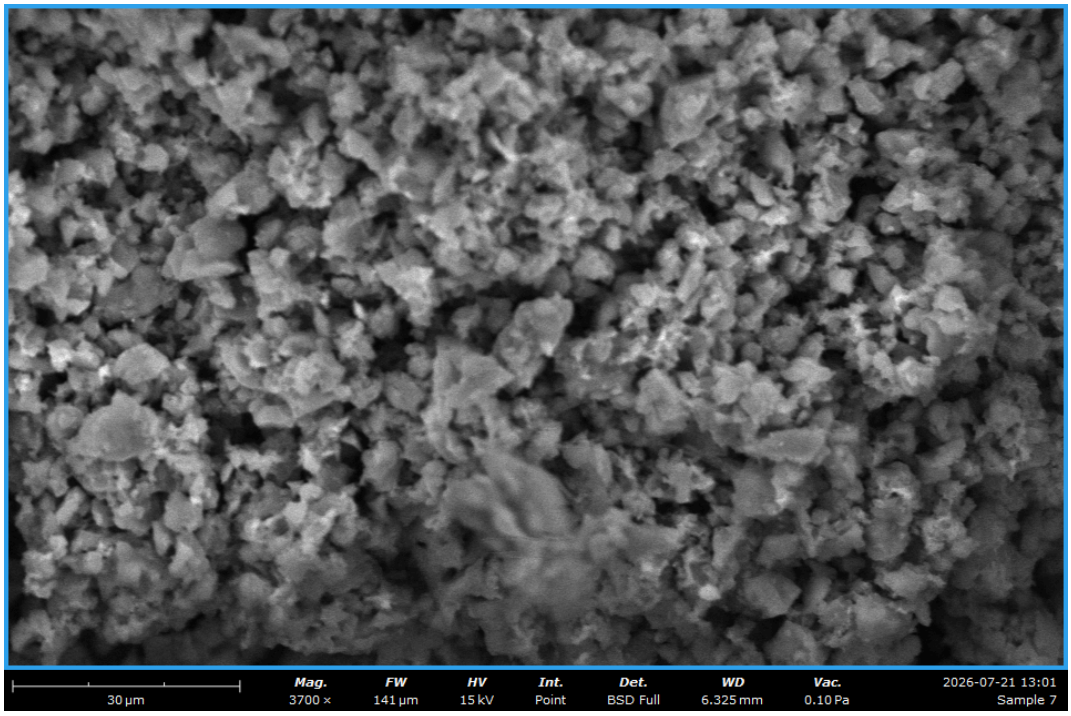


**Figure 9.** SEM micrograph of grafted Ti-PMO (3700×, 15 kV, BSD detector), showing irregular, aggregated particulate morphology with sizes ranging from roughly 1-10 µm.

**SEM** imaging of the grafted Ti-PMO showed the expected particulate morphology consistent with a mesoporous material.

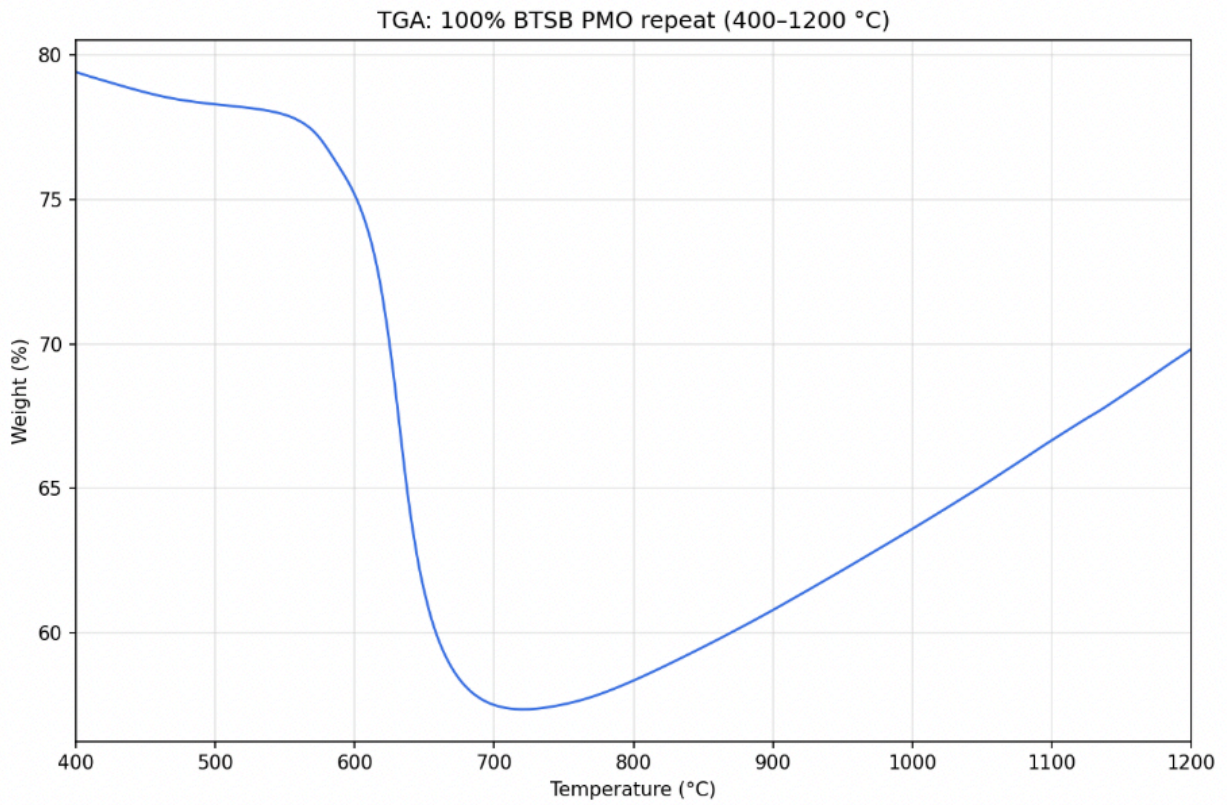


**Figure 10.** TGA of 100% BTSB PMO from 400-1200°C (30°C/min, initial mass 3.29493 mg).

The sample was heated at 30 °C/min under the standard TGA ramp (initial mass 3.29493 mg). The sample mass remained relatively stable from 400 °C (79.4% of initial mass) before undergoing a major decomposition step, with the fastest rate of mass loss occurring near 620–720 °C. The weight reaches a minimum of ~57.3% around 720 °C. Beyond around 720 °C, oxidation of the sample occurred, increasing the mass [11].

### 3.3 Photocatalytic performance: RhB degradation

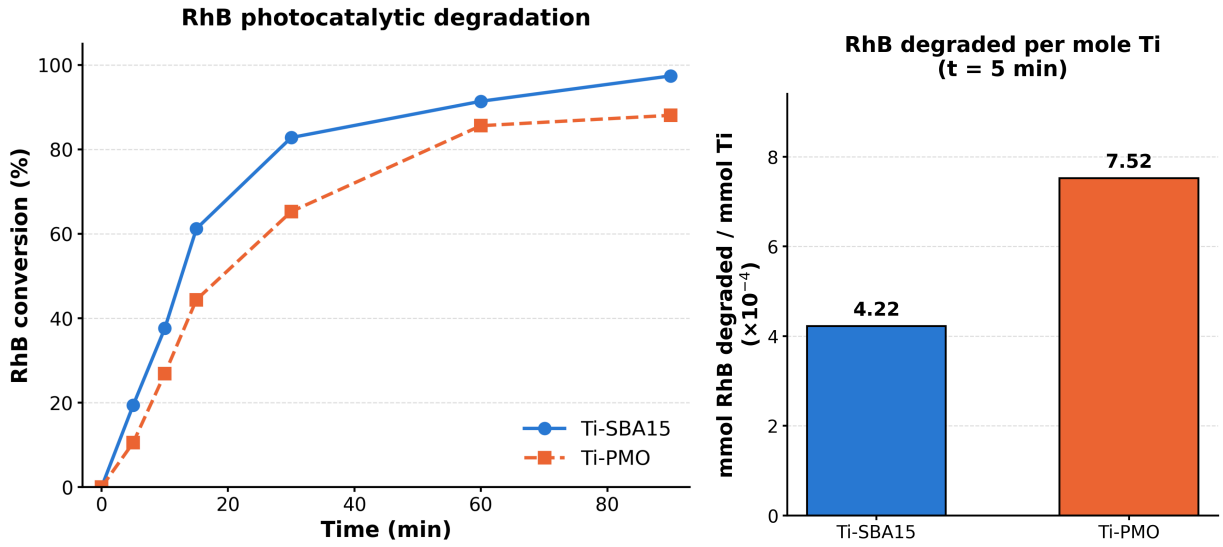


**Figure 11.** Photocatalytic degradation of Rhodamine B (RhB) by Ti-SBA15 and Ti-PMO over 90 min (left), and RhB degraded per mole of Ti at t = 5 min (right).

Ti-PMO degrades 1.78x more RhB per mole of Ti than Ti-SBA15 despite having 2.5x less Ti loading, indicating higher intrinsic activity per Ti site. Ti-SBA15 reaches near-complete conversion (97.4%) faster than Ti-PMO (88.1% at 90 min), reflecting its higher total Ti loading.

**Table 1.** Comparison of Ti loading and photocatalytic kinetics for Ti-SBA and Ti-PMO.

| Material | % Ti | Initial Rate (mg/L·min) | Initial TOF ($min^{-1}$) | Overall TOF ($min^{-1}$) |
|---|---|---|---|---|
| Ti-SBA | 9.75 | 0.084 | 0.086 | 0.023 |
| Ti-PMO | 3.96 | 0.083 | 0.21 | 0.069 |

Ti-PMO's per-site TOF is roughly 2.4x higher than Ti-SBA15's. The two catalysts degrade RhB at nearly identical raw rates early on (0.084 vs 0.083 mg/L·min), but the Ti-PMO does it with less than half the Ti content.

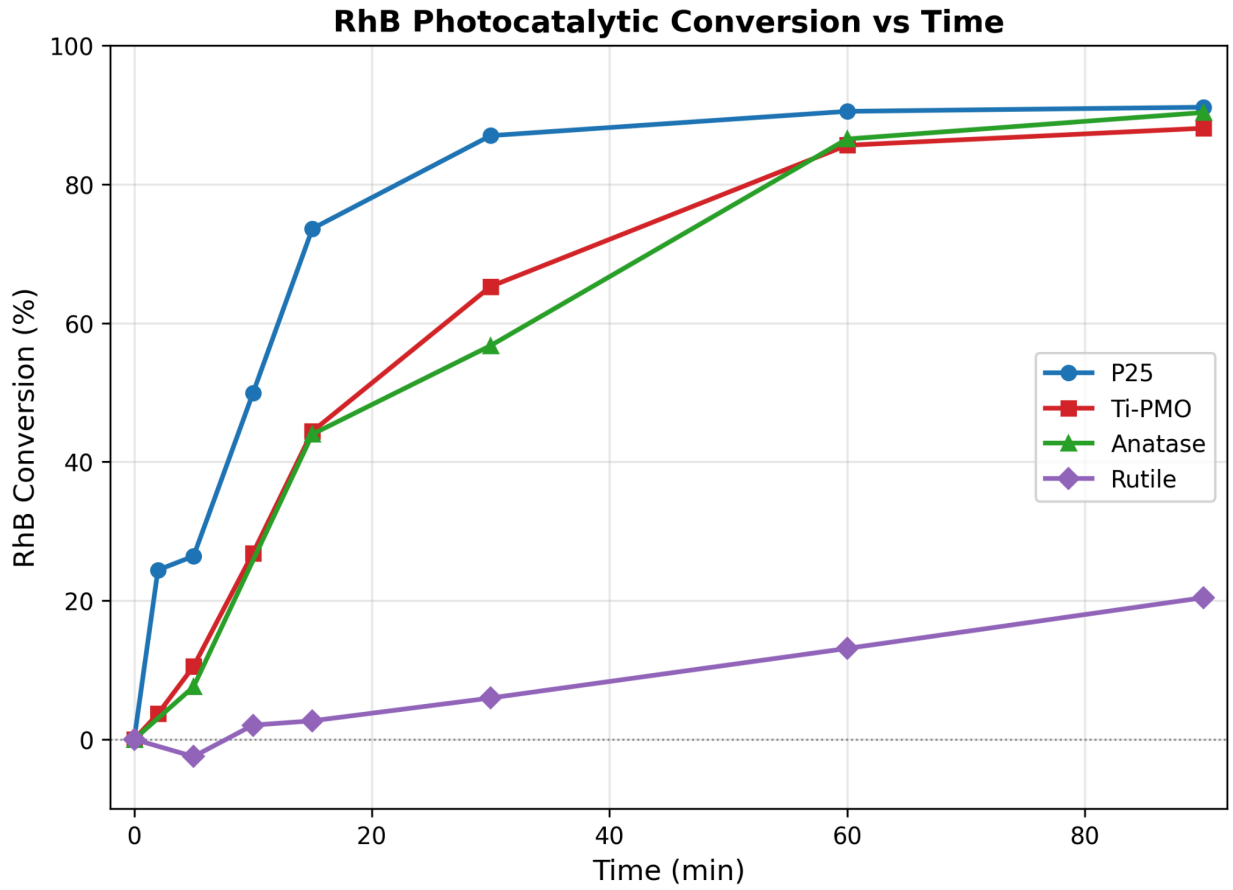


**Figure 12.** RhB photocatalytic conversion over time for Ti-PMO compared to benchmark TiO2 references (P25, anatase, rutile).

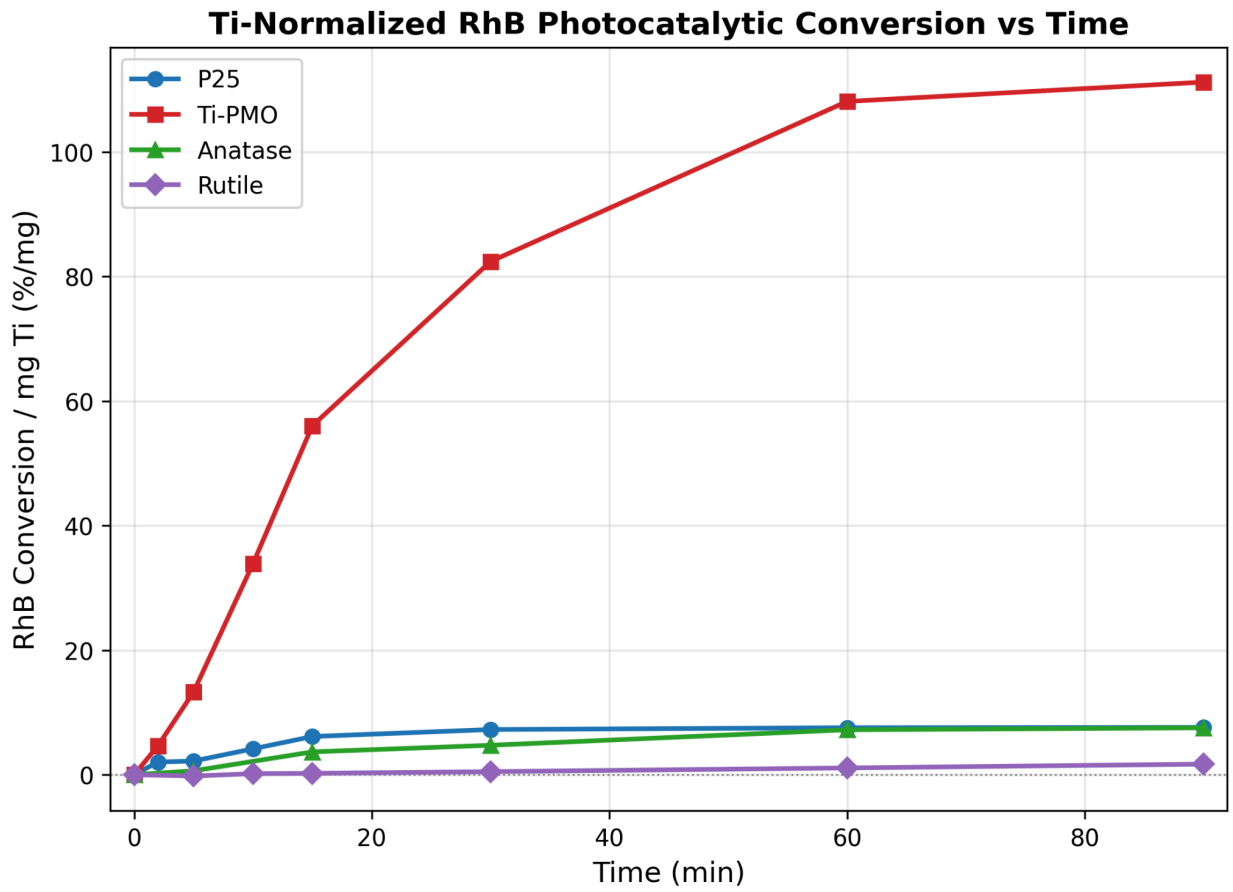


**Figure 13.** RhB conversion normalized to Ti mass for Ti-PMO versus P25, anatase, and rutile.

Compared to traditional Ti catalysts like P25 (a combination of the anatase and rutile TiO2 phases), as well as the pure anatase and rutile phases, the Ti-PMO offers substantially higher RhB removal capacity, reducing dye concentration by 65% before the photocatalytic degradation phase even begins, and achieves more consistent pseudo-first-order kinetics ($R^2$ = 0.95 vs. 0.79 for P25) while reaching comparable final conversion (88% vs. 91% at 90 min).

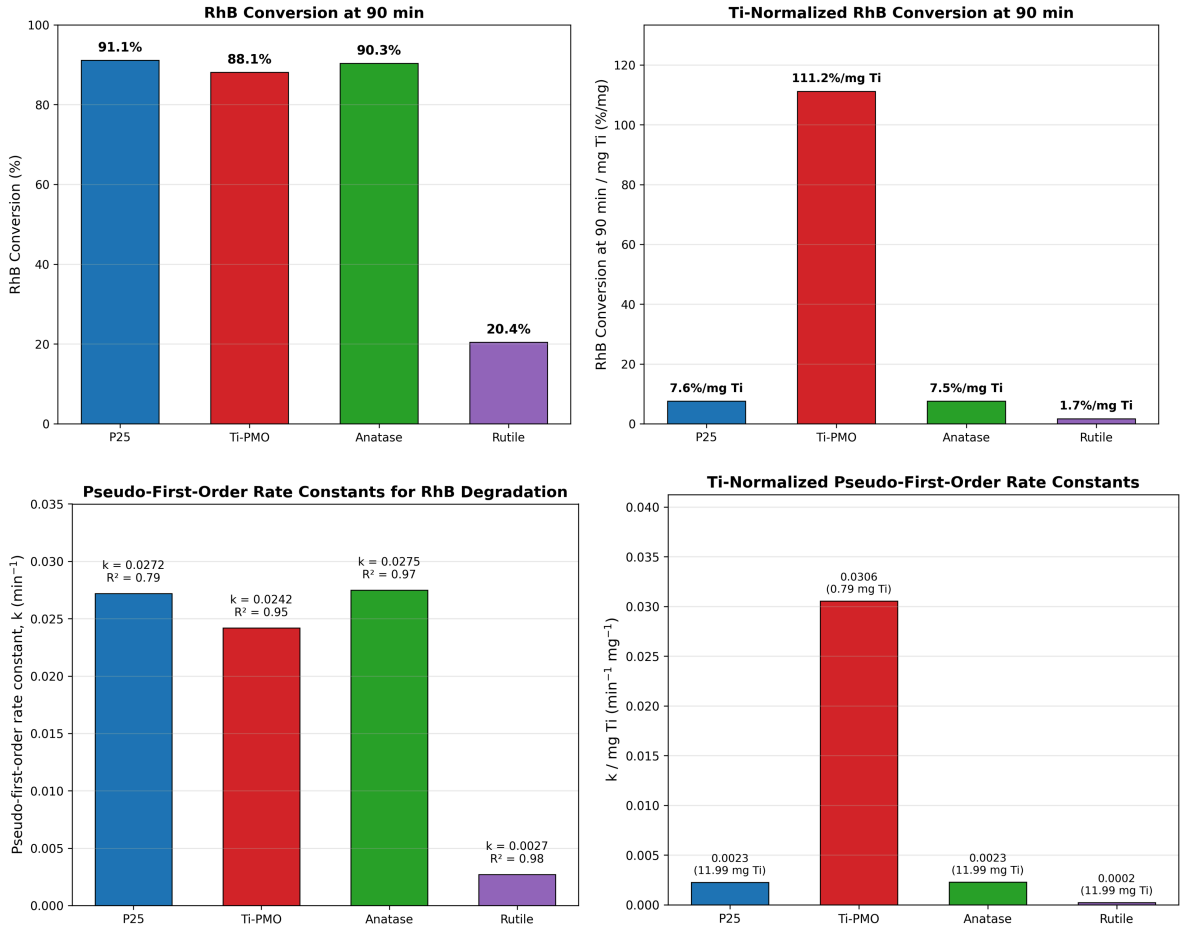


**Figure 14.** Percent photocatalytic conversion of RhB (initial concentration ≈ 8 mg/L, 20 mg catalyst, 20 mL solution) after 90 min of irradiation and pseudo-first-order rate constants (k) for P25 (blue), Ti-PMO (red), anatase (green), and rutile (purple). Charts on the right are normalized by % Ti loading for each catalyst.

Photocatalytic degradation of RhB was evaluated across P25, Ti-PMO, anatase, and rutile using two complementary sets of metrics: raw activity (percent conversion at 90 min and pseudo-first-order rate constant, k) and Ti-normalized activity (both metrics divided by mg of elemental Ti present in each 20 mg catalyst dose). The raw metrics show that P25, Ti-PMO, and anatase achieve comparable bulk performance (88-91% conversion, k = 0.024-0.028 $min^{-1}$), while rutile underperforms substantially, consistent with its known susceptibility to electron-hole recombination [20]. However, because P25, anatase, and rutile are 100% TiO2 (59.9 wt% Ti) while Ti-PMO contains only 3.96 wt% Ti, comparing raw activity alone obscures a critical difference in how efficiently each material utilizes its titanium content. Normalizing both metrics by Ti mass reveals that Ti-PMO achieves ~13-15x higher activity per milligram of Ti than P25 or anatase, indicating that a much larger fraction of Ti-PMO's titanium is catalytically accessible rather than buried in inert bulk structure. XPS and UV-Vis DRS characterization support this

interpretation, confirming isolated/highly dispersed Ti coordination and a higher energy absorption edge relative to bulk anatase/P25.

## 4. Discussion and Future Work

### 4.1 Discussion

This work set out to answer two questions. First, does a PMO support offer better hydrothermal stability than the current industry-standard SBA-15 support? Based on XRD and REELS evidence, the answer is yes: the PMO retains its ordered pore structure after 24 hours of hydrothermal treatment, while SBA-15 loses its higher-order structural features under the same conditions.

Second, can titanium be successfully grafted onto a PMO to create an active, well-defined catalyst, and how does it compare to the existing Ti-SBA15 catalyst? XRD, XPS, FTIR, REELS, and SEM together confirm that Ti-PMO was synthesized as intended, with isolated, fully oxidized Ti(IV) sites grafted onto an intact PMO framework. Photocatalytic testing using RhB degradation as a probe reaction showed that Ti-PMO achieves 2.4 times higher per-site catalytic activity than Ti-SBA15, despite containing 2.5 times less titanium.

A catalyst support that better withstands the wet, hot conditions generated by its own reaction has a longer usable lifetime. In an industrial SAF production process, using a PMO-based catalyst translates into fewer catalyst replacements, less production downtime, and a lower cost per liter of fuel produced [5, 17].

### 4.2 Future Work

Several next steps follow directly from this work:

- **Photoluminescence (PL) spectroscopy**, to directly investigate whether the aromatic PMO framework improves charge-carrier separation at titanium sites, testing the mechanistic hypothesis raised in Section 3.4 [2, 14].
- **Catalyst durability testing**, running the catalyst through repeated reaction cycles to assess how activity changes over realistic, extended operating timescales, rather than the single-pass tests used here [3, 22].
- **N2 physisorption (BET) analysis**, to quantify surface area, pore diameter, and pore volume before and after hydrothermal ageing, giving a numerical complement to the qualitative structural picture from XRD.
- **Testing Ti-PMO on the actual aldol condensation reaction** (CPO + FAL, rather than RhB degradation), to confirm that the per-site activity advantage seen with the RhB probe reaction translates to the reaction that actually matters for SAF production [6, 7, 9].

## Acknowledgements

Thank you to the Laidlaw Foundation for financing this research, to Mark Isaacs and Lucy Costley-Wood for their mentorship and guidance, and to Emily Feeke, Leonardo Da Silva Sousa, Oliver Hodson, and Zhaohong Ying from the UK Catalysis Hub for their help during this project.

### References

1. Isaacs, M. A., Drivas, C., Graf, A., et al. (2025). Understanding the chemical and electronic properties of sub-monolayer $TiO_2$ on high surface area silica for jet fuel synthesis applications. *Advanced Functional Materials, 36*, e02818. https://doi.org/10.1002/adfm.202502818
2. dos Santos-Durndell, V. C., Isaacs, M. A., Manayil, J. C., et al. (2025). Light or acid? Suppressing water deactivation in SAF production via phenyl-mediated charge transfer in WOx/ZrOx-functionalised PMOs. *Applied Catalysis O: Open, 209*, 207078. https://doi.org/10.1016/j.apcato.2025.207078
3. dos Santos-Durndell, V. C., Durndell, L. J., Isaacs, M. A., Lee, A. F., & Wilson, K. (2023). WOx/ZrOx functionalised periodic mesoporous organosilicas as water-tolerant catalysts for carboxylic acid esterification. *Sustainable Energy & Fuels, 7*, 1677–1686. https://doi.org/10.1039/D2SE01724E
4. Van Der Voort, P., Esquivel, D., De Canck, E., Goethals, F., Van Driessche, I., & Romero-Salguero, F. J. (2013). Periodic mesoporous organosilicas: From simple to complex bridges. *Chemical Society Reviews, 42*, 3913–3955. https://doi.org/10.1039/C2CS35222B
5. Baldenhofer, R., Jansen, L., van der Ham, A. G. J., Lange, J.-P., Kersten, S. R. A., & Ruiz, M. P. (2025). Cleared for take off? Technoeconomic analysis for the conversion of furfural to sustainable aviation fuel via aldol condensation. *Industrial & Engineering Chemistry Research, 64*(43), 20805–20819. https://doi.org/10.1021/acs.iecr.5c02229
6. Cueto, J., de la Calle, D., Alonso-Doncel, M. M., Giner, E. A., García-Muñoz, R. A., & Serrano, D. P. (2025). Enhanced production of jet fuel precursors via furfural/cyclopentanone aldol condensation by synergistic pairing TiO2 with nano-ZSM-5 zeolite. *Bioresource Technology, 418*, 131877. https://doi.org/10.1016/j.biortech.2024.131877
7. de la Calle, D., Cueto, J., Alonso-Doncel, M. M., García-Muñoz, R., & Serrano, D. P. (2026). *Production of precursors for sustainable aviation fuels through furfural/cyclopentanone aldol condensation boosted by TiO2-loaded dendritic ZSM-5 catalysts* [Data set]. Zenodo.
8. Zanuttini, M. S., et al. (2023). Production of a high molecular weight jet-fuel precursor from biomass derived furfural and 2-methylfuran using propyl sulfonic SBA-15 catalysts. *Applied Catalysis A: General, 665*, 119383.
9. Yevdokimova, O., Shcherban, N., Martinez-Klimov, M., Weydisch, R., Cueto, J., Alonso Giner, E., Eränen, K., Peuronen, A., Lastusaari, M., Russo, V., Mäki-Arvela, P., & Murzin,

D. Y. (2025). Synthesis of jet-fuel precursors from renewable biomass through aldol condensation of cyclopentanone and furfural on base catalysts. *Catalysis Today, 443*, 114962. https://doi.org/10.1016/j.cattod.2024.114962

10. Burleigh, M. C., et al. (2003). Mechanical and hydrothermal stabilities of aged periodic mesoporous organosilicas. *The Journal of Physical Chemistry B, 107*, 12628–12634. https://doi.org/10.1021/jp035189q
11. Esquivel, D., Jiménez-Sanchidrián, C., & Romero-Salguero, F. J. (2011). Comparison of the thermal and hydrothermal stabilities of ethylene, ethylidene, phenylene and biphenylene bridged periodic mesoporous organosilicas. *Materials Letters, 65*(10), 1460–1462. https://doi.org/10.1016/j.matlet.2011.02.037
12. Hunks, W. J., & Ozin, G. A. (2004). Periodic mesoporous organosilicas with phenylene bridging groups, 1,4-(CH2)nC6H4 (n = 0–2). *Chemistry of Materials, 16*, 5465–5472. https://doi.org/10.1021/cm048986p
13. Guo, W., Li, X., & Zhao, X. S. (2006). Understanding the hydrothermal stability of large-pore periodic mesoporous organosilicas and pure silicas. *Microporous and Mesoporous Materials, 93*(1–3), 285–293. https://doi.org/10.1016/j.micromeso.2006.03.009
14. Castanheira, B., Brochsztain, S., Otubo, L., & Teixeira, A. C. S. C. (2023). Periodic mesoporous organosilicas containing naphthalenediimides as organic sensitizers for sulfadiazine photodegradation. *Journal of Hazardous Materials, 443*, 130224. https://doi.org/10.1016/j.jhazmat.2022.130224
15. Ahadi, A., Alamgholiloo, H., Rostamnia, S., et al. (2019). Layer-wise titania growth within dimeric organic functional group viologen periodic mesoporous organosilica as efficient photocatalyst for oxidative formic acid decomposition. *ChemCatChem, 11*, 4803–4809. https://doi.org/10.1002/cctc.201900486
16. Inada, H., Morita, M., & Maeda, K. (2024). Stabilisation of molecular TiO4 species on the pore surface of mesoporous silica for photocatalytic H2 evolution. *Dalton Transactions, 53*, 13756–13763.
17. Jiang, Y., Seiple, T., Pierobon, F., Rosales Calderon, O., Tao, L., Sanyal, U., Biller, P., Yang, Z., Heyne, J. S., Ramasamy, K. K., & Wang, H. (2026). Feedstocks and processes for global-scale sustainable aviation fuel production. *Nature Reviews Clean Technology, 2*(8), 554–570. https://doi.org/10.1038/s44359-026-00190-1
18. Ismail, R., Alherbawi, M., Mariyam, S., McKay, G., & Al-Ansari, T. (2025). Catalytic pathways towards sustainable aviation fuel production from waste biomass: A systematic review. *Cleaner Engineering and Technology, 29*, Article 100927. https://doi.org/10.1016/j.ceja.2025.100927
19. Kazmi, W. W., Syed, M. W., Waqas, M., Bhatti, U. H., Omer, A., Ali, M., Zulqarnain, Kariim, I., Hussain, A., & Al-Khulaifi, F. M. (2026). A review on sustainable aviation fuel production via diverse biomass and waste-derived feedstocks and cutting-edge conversion technologies. *Biomass and Bioenergy, 212*, Article 109281. https://doi.org/10.1016/j.biombioe.2026.109281
20. Yang, L., Zhang, J., Tong, H., Li, X., Zhao, D., & Lan, K. (2025). Synthesis of mesoporous titania nanomaterials for evolving photocatalytic applications. *Advanced Energy Materials, 15*(44), e02405. https://doi.org/10.1002/aenm.202502405

21. Park, S. S., Santha Moorthy, M., & Ha, C.-S. (2014). Periodic mesoporous organosilicas for advanced applications. *NPG Asia Materials, 6*, e96. https://doi.org/10.1038/am.2014.13
22. Doustkhah, E., Mohtasham, H., Hasani, M., Ide, Y., Rostamnia, S., Tsunoji, N., & Assadi, M. H. N. (2020). Merging periodic mesoporous organosilica (PMO) with mesoporous aluminosilica (Al/Si-PMO): A catalyst for green oxidation. *Molecular Catalysis, 482*, 110676. https://doi.org/10.1016/j.mcat.2019.110676